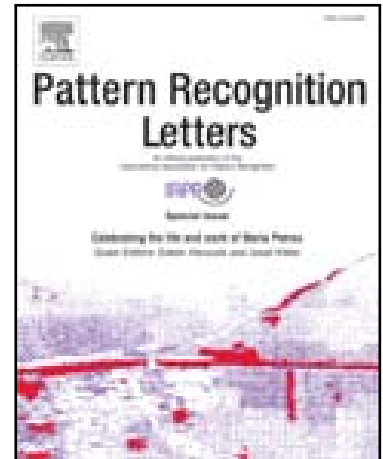


Evaluating the Performance of Face Sketch Generation using
Generative Adversarial Networks

M S Sannidhan , G AnanthPrabhu , David E. Robbins ,
Charles Shasky

PII: S0167-8655(19)30283-1
DOI: <https://doi.org/10.1016/j.patrec.2019.10.010>
Reference: PATREC 7658



To appear in: *Pattern Recognition Letters*

Received date: 22 September 2019
Revised date: 9 October 2019
Accepted date: 12 October 2019

Please cite this article as: M S Sannidhan , G AnanthPrabhu , David E. Robbins , Charles Shasky ,
Evaluating the Performance of Face Sketch Generation using Generative Adversarial Networks, *Pat-
tern Recognition Letters* (2019), doi: <https://doi.org/10.1016/j.patrec.2019.10.010>

This is a PDF file of an article that has undergone enhancements after acceptance, such as the addition of a cover page and metadata, and formatting for readability, but it is not yet the definitive version of record. This version will undergo additional copyediting, typesetting and review before it is published in its final form, but we are providing this version to give early visibility of the article. Please note that, during the production process, errors may be discovered which could affect the content, and all legal disclaimers that apply to the journal pertain.



Evaluating the Performance of Face Sketch Generation using Generative Adversarial Networks

Sannidhan M S^{a,*}, AnanthPrabhu G^b, David E. Robbins^c, and Charles Shasky^d

^aNMAM Institute of Technology, (Visvesvaraya Technological University, Belagavi), Nitte, Karnataka, India

^bSahyadri College of Engineering and Management, (Visvesvaraya Technological University, Belagavi), Adyar, Karnataka, India

^cSchool of Public Health, Department of Health Informatics and Information Management, Samford University, Birmingham, AL, USA

^dVisiting Professor, Department of Health Administration, VCU/KMU EMHA Program, Medical College of Virginia, Virginia Commonwealth University, Richmond, VA, USA

ABSTRACT

One of the most significant and widely used methods for identifying a culprit in the field of forensic science is generating a sketch of the suspect from descriptions given by an eyewitness to the crime. However, there is a high level of uncertainty in recognizing an individual solely from a sketch. Recognition of sketches based on photos of an individual is non-trivial, as there are differences between the domain features of a sketch and a photo. To streamline this process, this article presents a methodology for generating a colored photo from a sketch, which can then be used for identification using a variety of classification techniques. Implementation of the proposed method involves a trained Convolution Neural Network for sketch generation paired with a conditional Generative Adversarial Network's pix2pix model for color photo generation. Experimental results of the work are validated using standard datasets, and the proposed model achieved a minimum average rate of 65% similarity index value on all employed datasets with a training efficiency of more than 98% in every epoch level.

Keywords: adversarial network, convolution neural network, deep learning, sketch to photo matching, sketch generation, photo generation

* Corresponding author.: e-mail: sannidhan@nitte.edu.in

Driven by technological advances, face recognition systems have gained a wide scope of applications across the globe. In the application of face recognition algorithms for forensic science, sketch identification of a culprit is one of the most highly used methods. Sketch identification is used in crime investigations, in which an eyewitness to a crime scene is asked to recollect the features of a culprit and an expert sketch artist will generate a sketch according to the description given by the witness [1]. Later, those generated sketches are compared with a set of images already available within the database. Sketches are generated by three commonly used techniques [2]: 1) a skilled artist produces a viewed sketch by referring a photo; 2) a skilled artist produces a forensic sketch using an eyewitness description; and 3) a sketch is generated using some standard application software. Two examples of computer-generated sketches and their corresponding photos are depicted in Fig. 1, taken from the Chinese University of Hong Kong (CUHK) dataset.



Fig. 1. Two photographs and their corresponding sketch depictions, taken from the CUHK dataset

One major downfall of sketches when compared to colored photos is that sketches lack the rich details pertaining to a person's skin color and texture, as well as certain unique facial features. Because of these missing features, it is difficult for traditional face identification algorithms to identify and match suitable sketch depictions with corresponding photos [1, 2]. Nonetheless, due to the advancements in the field of computer vision, this task can be accomplished using the techniques of deep learning [3, 4]. One such development is Generative Adversarial Network (GAN), which uses deep learning to generate a color photo as an output from a sketch, making the identification process easier through classification [4, 29]. To this end, our research has emphasized the use of conditional Generative Adversarial Network (cGAN) to generate colored photo images from the available facial sketches, enabling efficient classification that avoids cross domain problems in sketch identification [6]. The accuracy of the image generated by GAN depends on the quality of the sketches used to train the adversarial network. So, to ensure a better training process, we propose the fusion of two different deep learning systems to generate an accurate color photo image. A content network with an inception module and a Convolution Neural Network (CNN) of two and three layers are trained to generate enhanced sketches; these sketches are then used to train a cGAN with a Pix2Pix module for the translation of sketches into color photos. Evaluation of the proposed technique was conducted using standard data sets available to the research community and the achieved results were validated using standard evaluation metrics used for image [7].

2. Motivation

The research is motivated by the state-of-the-art techniques presented by Fernandes et al. [5] in the area of composite sketch matching. Deep learning was first applied by Fernandes et al. to match face images with composite sketches [9]. The research idea presented by Fernandes et al. is considered foundational in the field of computer vision. Fernandes et al. presented the first composite sketch matching approach with images captured from the unmanned aerial vehicle [15]. This approach was patented and has been successfully used by law enforcement agencies in India to find frequent offenders [20].

The proposed system is broadly divided into two stages: 1) sketch generation through trained CNN; and 2) color photo generation through trained cGAN. The working methodology of the system is presented below in Fig. 2.

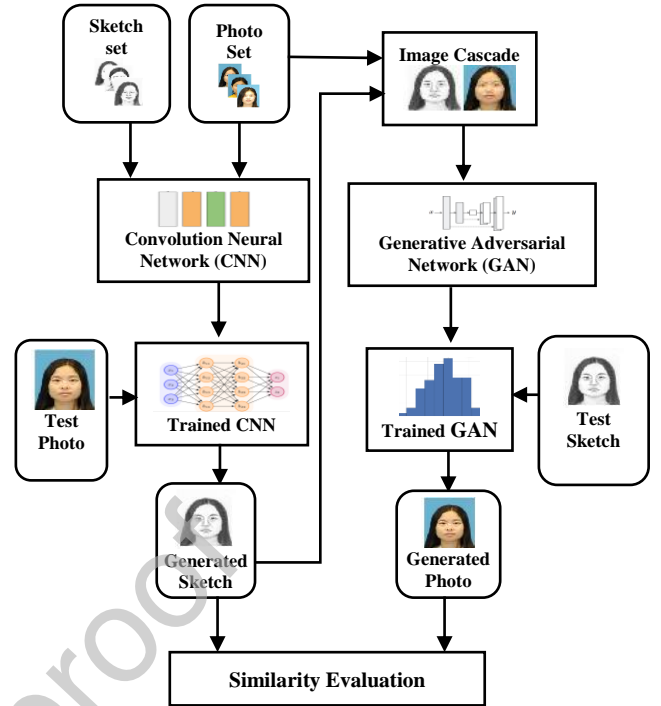


Fig. 2. Architecture of the proposed system

3.1. Sketch Generation

3.1.1. Pre-processing

In this stage, we calculate the centre point value of eyes in both photo images and sketch images [8]. Extracted values are used for the purpose of image alignment. This stage is highly significant for training the network, which requires the extraction of various points of interest from the photo images and sketches.

3.1.2. Creation of a Content image

P_i , a pre-processed color photo achieved from the previous stage, is fed as input to the content network to produce a content image C_i . C_i is an outline of the facial photo P_i , with some essential features of the entire face region representing the eyes, nose, mouth region, and an area representing hair. The working of the content network is presented in Fig. 3.

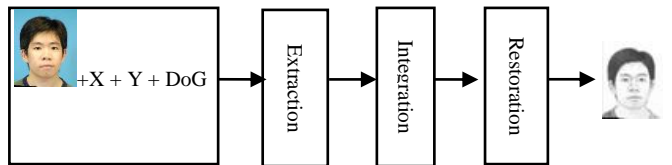


Fig. 3. Workflow describing the creation of the content image

In the above process, a photo along with channels related to x and y coordinates and information corresponding to the Difference of Gaussian (DoG) value of an image is supplied to the content network. Consolidated information pertaining to a photo undergoes three steps: 1) extraction, 2) integration, and 3) restoration.

Extraction of features is performed using a two-layered inception module (inc_module) [30]. This module extracts features in three level filters of order 1×1 , 3×3 , and 5×5 sequentially. Extracted features are fed into the three-layer CNN, integrating extracted features from three filters of variable size in normalized form, resulting in 1×1 uniform order. Integrated

image C_i , with the order of 3×3 . The resulting content image C_i may have information loss, with respect to the sketch S_i . This loss is calculated according to equation 1:

$$L = \frac{1}{n} \sum_{k=1}^n |C_k - S_k| \quad (1)$$

3.1.3. Target Estimator

This module is dedicated to training the photo-sketch sets required for training the CNN. The process begins by dividing both photos and sketches into a grid of pixels, which will later divide into non-overlapping patches of order 16×16 . The process of the target estimator is presented in Fig 4.

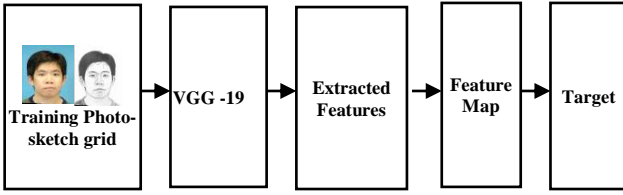


Fig. 4. Workflow describing the process of Target Estimator

For the process depicted above, the VGG-19 network has five layers of CNN, with each layer assigning a 19-weight value. This network trains itself with features corresponding to 16 non-overlapping patches of the photo images and their sketches. Patches of photos are mapped with the corresponding patches of sketches having the lowest Mean Square Error (MSE) between them [10-13]. This process ensures the necessary grouping of the target sketch to be generated for a photo image.

3.1.4. Generation of Sketch

This stage generates the final sketch required for a test photo, using the content image generated and the sketch target. It combines the content image and the mapped features of the target to derive an accurate sketch. Equation (2) presents the mathematical formulation for the working procedure: [9]

$$F_i = \psi(C_i, T_i) \text{ for } i = \{1, 2, 3, \dots, n\} \quad (2)$$

Here, F_i represents the final generated sketch of an i th image; ψ is the generator function which maps content image C_i and target image T_i into a single sketch image.

3.2. Color Photo Image Generation

3.2.1. Cascading Images

This step prepares the data sets for training the Pix2Pix model of an adversarial network. Here, we cascade every photo image with its corresponding sketch image to achieve a concatenated image. This process is depicted in Fig. 5.



Fig. 5. Cascading process

$$T_k = C_a(P_k, S_k) \quad (3)$$

T_k Represents the required training image for the k th image set; C_a represents the concatenation function that concatenates a photo image P_k and sketch image S_k .

3.2.2. Training Conditional GAN Pix2Pix Model

Training cGAN is associated with the training of two important modules: discriminator training and generator training. The following subsections provide detailed explanation on these two modules.

3.2.2.1. Discriminator Training

The discriminator training uses the generated output image. Here we consider the sketch as input and the generated color photo as output. Upon receiving the generated photo, the discriminator examines the cascaded input sketch/target photo image pair and input sketch/generated output pair and delivers a guess corresponding in terms of their SSIM. Based on the accuracy of this outcome, the discriminator improves its learning efficiency by adjusting the weights with respect to error of classification connected to input sketch/generated photo image pair and input sketch/target photo image pair. In parallel, it also makes the adjustment of weights in the generator. The entire architecture of the discriminator [14-16] training is displayed in Fig. 6 below and is mathematically formulated in Equation 4:

$$D(I, O) \rightarrow \begin{cases} \text{Error weights calculated through MSE} \\ 0 \text{ if } P = 1 \end{cases} \quad (4)$$

I represents the input image; O represents the output image; and MSE is the Mean Square Error of I and O . P is the probability value calculated for I and O .

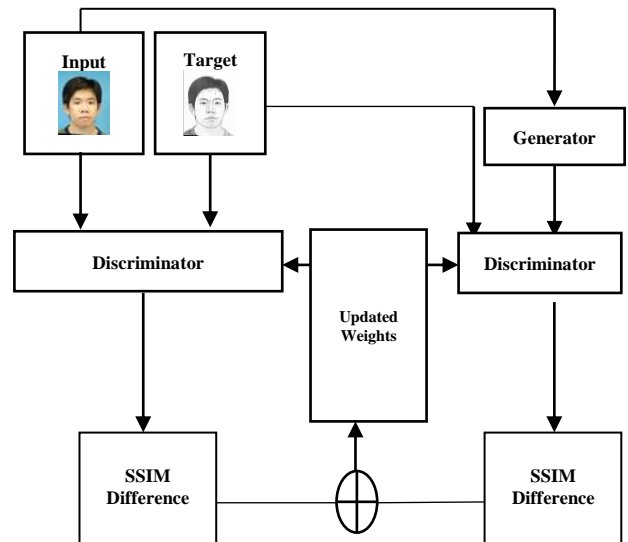


Fig. 6. Workflow of discriminator training

3.2.2.2. Generator training

A generator is also trained in tandem with the discriminator. We make use of this generator to supply a sketch of $256 \times 256 \times 3$ (3 is the channels of RGB values). It initially performs the sequence of encoding operations, which expresses the smaller level of representation with an order of $2 \times 2 \times 512$ of

The training process of the generator is very similar to the discriminator training, with some small variations. Here the generator accepts the input sketch image and produces a color photo as output. The generated photo and initial sketch are fed to the discriminator to compare the accuracy of the initial guess. The accuracy of the generated photo is also compared with the target photo. The calculated difference is used to update the generator weights for better accuracy of generation. The generator training process [14-16] is presented in Fig. 7, and the mathematical formulation representing the process is described in Equation 5:

$$G(I, N) \rightarrow O \quad (5)$$

I represents the input image; N represents the noise factor; and O represents the output image.

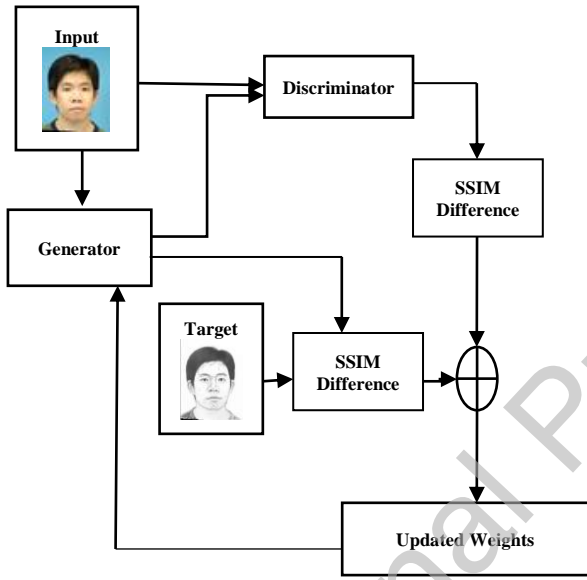


Fig. 7. Workflow of generator training

3.2.3. Functioning of Generative Adversarial Network

The GAN function maximizes the probability of the generator and the discriminator, which is formulated using Equation 6[31]:

$$P_{GAN}(G, D) = E_{I,O}[\log D(I, O)] + E_{I,N}[\log(1 - D(I, G(I, N)))] \quad (6)$$

$P_{GAN}(G, D)$ is a probability function of the GAN output, with respect to G and D modules; $E_{I,O}$ is an expected value of input I and output O ; $E_{I,N}$ is an expected value of input I and noise factor N .

The mathematical formulation for an expected value function is formulated as per Equation 7: [16-19]

$$E(m, n) = \sum \sum m_i X n_i X P(m_i, n_i) \quad (7)$$

Where m and n are the parameters for an expected function; E and P are the probability functions of the two parameters, m and n .

formulated in Equation 8:

$$L(G) = E_{I,O,N}[(1 - G(I, N))] \quad (8)$$

4. Results and Discussion

All experimental results are carried out on a GPU system containing Dual NVIDIA Tesla P100 Graphical Processing Unit, with 3584 cores and a maximum of 18.7 Teraflops running on Dual Intel Xeon E5-2609V4 8C 1.7GHz 20M 6.4GT/s with 128GB primary memory. To validate the results, we have used three datasets: CUHK, Celebs and PRIP-HDC [21-26].

4.1. Data preparation

4.1.1. Data preparation for training content network

All the photo-sketch pairs required for the purpose of training are scaled to a size of 288×288, aligned with respect to the eyes of an image set

4.1.2. Data preparation for training pix2pix model

Every photo and sketch required for this model is scaled to a value of 300×300, for uniformity.

4.2. Visual Presentation of Results

4.2.1. Result produced by a CNN sketch generator



Fig. 8. The first column presents the input photo image; the second column presents the original sketch image; and the third column presents the generated sketch using trained CNN.

4.2.2. Result produced by a cGANpix2pix photo image generator



Fig. 9. The first column represents the sketch generated using the CNN; the second column shows the original photo; and the third column shows the image that is being generated using cGAN.

4.3. Similarity evaluation of generated image

PSNR (Peak Signal to Noise Ratio)

$$PSNR = 10 \log_{10} \left(\frac{p_val^2}{MSE} \right) \quad (9)$$

Where p_val represents the peak value of the signal and is considered to be 256 for a color image. A higher PSNR value corresponds with a greater image quality.

$$MSE = \frac{\sum_P \sum_Q [PI_1(i,j) - PI_2(i,j)]^2}{P * Q} \quad (10)$$

Where P, Q correspond to order of the image matrix; PI_1 and PI_2 represent the actual image and the generated image, respectively. A lower MSE value corresponds with a greater image quality.

SSIM (Structural Similarity Index)

$$SSIM_{l,m} = \frac{(2\mu_l\mu_m + C1)(2\sigma_{lm} + C2)}{(\mu_l^2 + \mu_m^2 + C1)(\sigma_l^2 + \sigma_m^2 + C2)} \quad (11)$$

Where μ calculates the average value of two parameters; σ calculates the variance of two values; and l, m represent the coordinate values.

4.3.1. Quality Metric and Accuracy Analysis

Table1. Quality metric evaluation of generated photo images from cGAN pix2pix, trained using sketches generated through CNN

| Dataset Name | Average SSIM↑ | Average PSNR↑ | Average MSE↓ |
|---------------------------------|---------------|---------------|--------------|
| CUHK (Composite Sketch- Photo) | 0.6742 | 18.25 | 1197 |
| PRIP-HDC (Viewed Sketch- Photo) | 0.6484 | 17.816 | 1266.7 |
| Celebs (Photo images) | 0.7029 | 28.515 | 1120.4 |

Table2. Quality metric evaluation of generated photo images from cGAN pix2pix, without using sketches generated through CNN for training

| Dataset Name | Average SSIM↑ | Average PSNR↑ | Average MSE↓ |
|---------------------------------|---------------|---------------|--------------|
| CUHK (Composite Sketch- Photo) | 0.5882 | 15.969 | 1954 |
| PRIP-HDC (Viewed Sketch- Photo) | 0.5619 | 14.512 | 2177.3 |
| Celebs (Photo images) | 0.615 | 24.932 | 1875.63 |

Experimental results depicted in Table 1. and Table 2. Confirms that the quality of photos generated from the sketches of trained CNN is better than the actual sketches available in the dataset. Hence sketches generated through CNN plays a vital role in training cGAN

Table 3. Training accuracy percentage and loss percentage of cGAN pix2pix photo image generator for different datasets

| Dataset Name | Epoch level | % Accuracy | % Loss |
|---------------------------------|-------------|------------|--------|
| CUHK (Composite Sketch- Photo) | 100 | 97.95 | 2.05 |
| | 200 | 98.05 | 1.95 |
| | 300 | 98.1 | 1.9 |
| | 400 | 98.17 | 1.83 |
| PRIP-HDC (Viewed Sketch- Photo) | 100 | 97.44 | 2.56 |
| | 200 | 97.75 | 2.25 |
| | 300 | 97.8 | 2.2 |
| | 400 | 97.85 | 2.15 |
| Celebs (Photo images) | 100 | 98.26 | 1.74 |
| | 200 | 98.28 | 1.72 |
| | 300 | 98.28 | 1.72 |
| | 400 | 98.31 | 1.69 |

Results achieved in Table 3. Confirms that an higher rate of training accuracy is achieved across the datasets with a minimal amount of loss incurred

4.4.1. Analysis of various quality metrics

SSIM Analysis

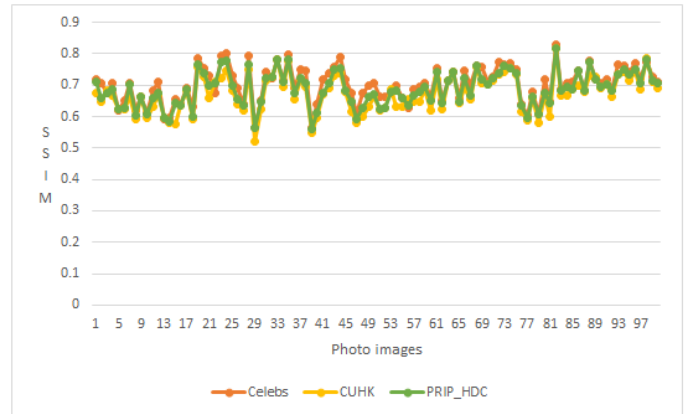


Fig. 10. Plot representing the SSIM values of different photo images

PSNR Analysis

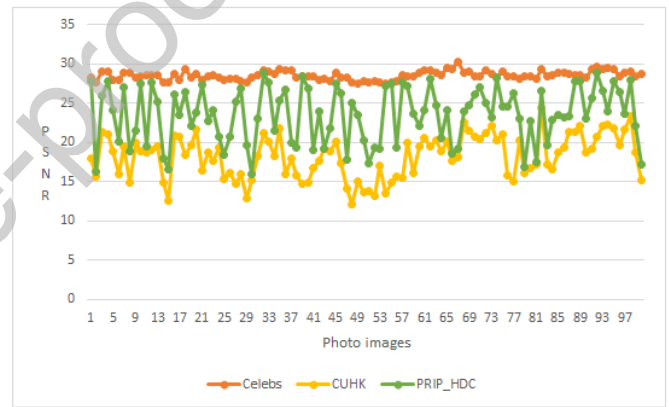


Fig. 11. Plot representing the PSNR values of different photo images

MSE Analysis

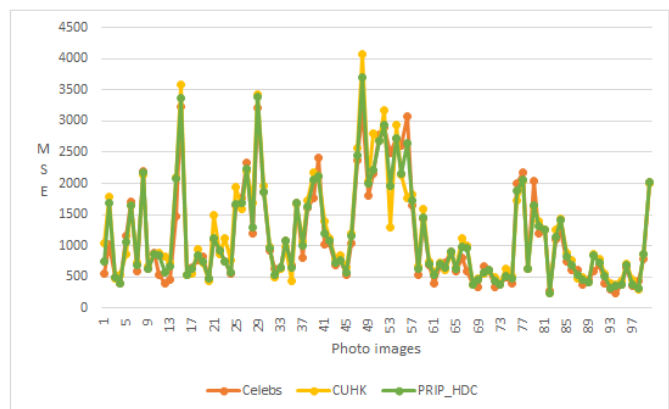


Fig. 12. Plot representing the MSE values of different photo images

4.5. Analysis of Training Accuracy

Under this section, we present the accuracy analysis of cGAN training under four different epochs level: 100,200,300 and 400 respectively for all the three different datasets.

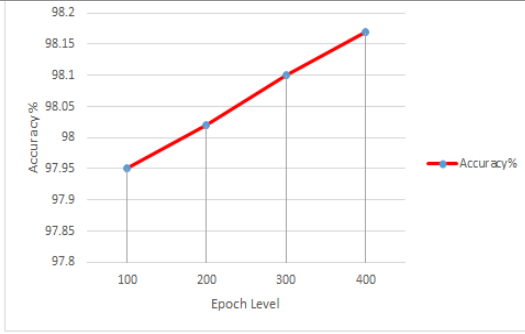


Fig. 13. Training accuracy of CUHK dataset

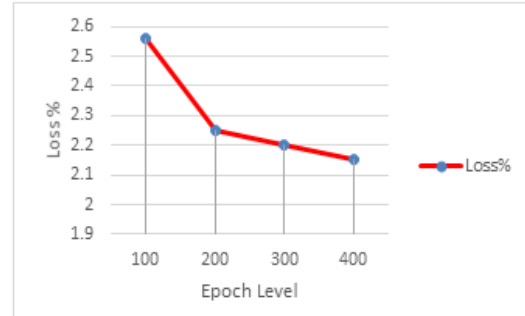


Fig. 17. Loss incurred in training PRIP-HDC dataset

Training Accuracy for PRIP-HDC dataset

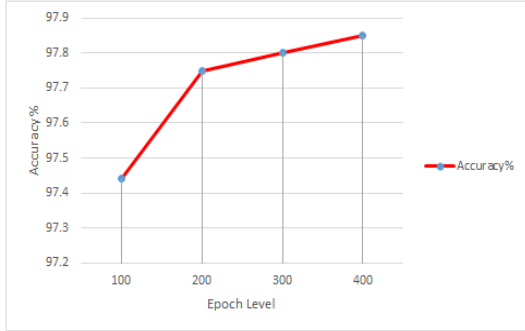


Fig. 14. Training accuracy of PRIP-HDC dataset

Loss incurred in training Celebs dataset

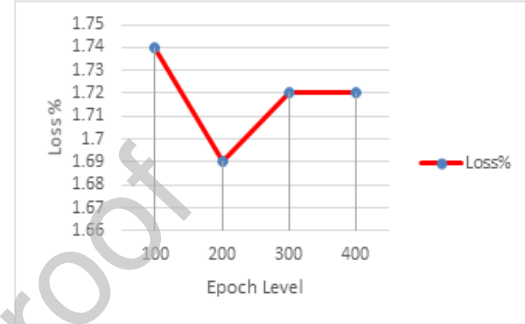


Fig. 18. Loss incurred in training Celebs dataset

Training Accuracy for Celebs dataset

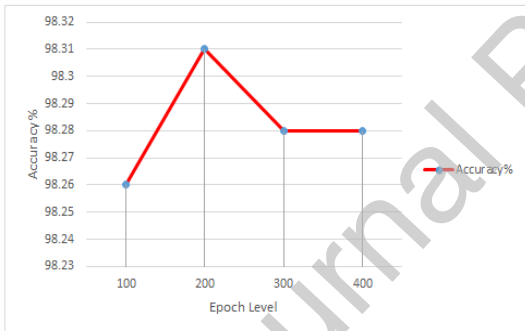


Fig. 15. Training accuracy of Celebs dataset

4.6. Analysis of Training Loss Incurred

Under this section, we present the Loss percentage incurred in cGAN training under four different epochs level: 100,200,300 and 400 respectively for all the three different datasets.

Loss incurred in training CUHK dataset

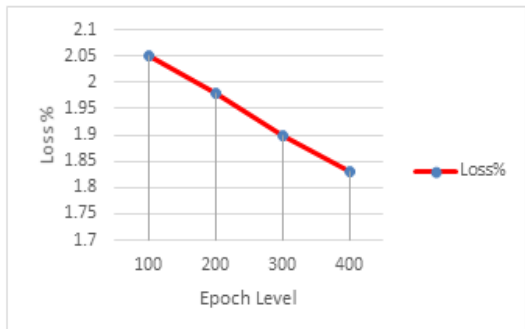


Fig. 16. Loss incurred in training CUHK dataset

4.7. Comparative Analysis

Table 4. Comparison of proposed system with other standard systems

| Method | PSNR | SSIM |
|---|---------|--------|
| Lu.et.al [33] | 15.9439 | 0.5785 |
| Zhao, j. et. al [34] | 16.3069 | 0.5790 |
| Proposed system without CNN generated sketches for training | 18.471 | 0.5883 |
| Proposed system with CNN generated sketches for training | 21.527 | 0.6751 |

Proposed system's PSNR and SSIM is compared with other existing systems as show in Table. 4 and it indicates that proposed system is comparatively better.

5. Conclusion

In this study, we attained our original objective of generating a colored photo image from a sketch input, using a combination of the CNN and cGAN pix2pix models. Significantly, this technique improves the accuracy of generated sketches and color photos. Through this we have further validated the dual application of deep learning to generate both sketches and photo images. Comparing the maximum average rate of similarity index value of 65% (Table 1) vs 61.5% (Table 2) confirms that sketches generated through CNN plays an important role in generating photos of better quality. Table 3 depicts the accuracy and loss percentage of training cGAN for up to 400 epochs, and the achieved results confirm that we have achieved a minimum accuracy of 97.85% and a maximum loss of 2.15% for 400 epochs on all the trained datasets. Our work was implemented and evaluated in Python, and open source programming language. One potential drawback of the proposal is that training of viewed sketches requires the application of image pre-processors.

6. Future Work

In the United States, estimates of healthcare fraud ranges between three and ten percent of all billed services. The United

8.12% rate [27]. For United States taxpayers this equates to about \$31.62 billion a year [28]. Credentialing of healthcare providers may include photo identification prior to validation of identity and enrollment into the payment system. Ongoing investigations and court proceedings yield facial sketches of criminal suspects. Convicted perpetrators of crimes may have facial sketches and photos in data files. These sketches and photos might then be compared to existing and validated photos of healthcare providers residing in health claims payer databases. Comparing generated photos from sketches or actual photos to validated provider photos prior to the payment of healthcare claims may be a valuable tool in identifying and reducing healthcare claims payment fraud by stolen healthcare provider identity methods. Implementing this fraud detection technology may be a valuable first step in reducing fraudulent and wasteful healthcare payments.

In future, this research can be improved by seeking a sketch conversion technique to improve the efficiency of the existing CNN. This work can also be extended for generating the photos with morphological variations. Further, while carrying out an exhaustive review under this research area, we have discovered the application of transfer learning approach for efficient classification. Hence in future, there is a high scope for implementing a transfer learning approach over cGAN for classification of photos available in a large dataset.

References

- [1] Kokila, R., Sannidhan, M. S., &Bhandary, A. (2017, March). A study and analysis of various techniques to match sketches to Mugshot photos. In *2017 International Conference on Inventive Communication and Computational Technologies (ICICCT)* (pp. 41-44). IEEE.
- [2] Kokila, R., Sannidhan, M. S., &Bhandary, A. (2017, September). A novel approach for matching composite sketches to mugshot photos using the fusion of SIFT and SURF feature descriptor. In *2017 International Conference on Advances in Computing, Communications and Informatics (ICACCI)* (pp. 1458-1464). IEEE.
- [3] Chen, C., Tan, X., & Wong, K. Y. K. (2018, March). Face sketch synthesis with style transfer using pyramid column feature. In *2018 IEEE Winter Conference on Applications of Computer Vision (WACV)* (pp. 485-493). IEEE.
- [4] Isola, P., Zhu, J. Y., Zhou, T., &Efros, A. A. (2017). Image-to-image translation with conditional adversarial networks. In *Proceedings of the IEEE conference on computer vision and pattern recognition* (pp. 1125-1134).
- [5] L Fernandes, S., & G Bala, J. (2017). A novel decision support for composite sketch matching using fusion of probabilistic neural network and dictionary matching. *Current Medical Imaging Reviews*, 13(2), 176-184.
- [6] Galea, C., &Farrugia, R. A. (2017). Matching software-generated sketches to face photographs with a very deep CNN, morphed faces, and transfer learning. *IEEE Transactions on Information Forensics and Security*, 13(6), 1421-1431.
- [7] Pallavi, S., Sannidhan, M. S., Sudeepa, K. B., &Bhandary, A. (2018, September). A Novel Approach for Generating Composite Sketches from Mugshot Photographs. In *2018 International Conference on Advances in Computing, Communications and Informatics (ICACCI)* (pp. 460-465). IEEE.
- [8] Wang, X., & Tang, X. (2008). Face photo-sketch synthesis and recognition. *IEEE Transactions on Pattern Analysis and Machine Intelligence*, 31(11), 1955-1967.
- [9] Fernandes, S. L., &Bala, G. J. (2016). ODROID XU4 based implementation of decision level fusion approach for matching computer generated sketches. *Journal of computational science*, 16, 217-224.
- [10] Zhou, H., Kuang, Z., & Wong, K. Y. K. (2012, June). Markov weight fields for face sketch synthesis. In *2012 IEEE Conference*
- [11] Mehdiipour Ghazi, M., & Kemal Ekenel, H. (2016). A comprehensive analysis of deep learning based representation for face recognition. In *Proceedings of the IEEE conference on computer vision and pattern recognition workshops* (pp. 34-41).
- [12] Zeng, Y., Cai, X., Chen, Y., & Wang, M. (2017, July). An accurate and efficient face recognition method based on hash coding. In *2017 13th International Conference on Natural Computation, Fuzzy Systems and Knowledge Discovery (ICNC-FSKD)* (pp. 20-23). IEEE.
- [13] Wang, Y., Bao, T., Ding, C., & Zhu, M. (2017, June). Face recognition in real-world surveillance videos with deep learning method. In *2017 2nd International Conference on Image, Vision and Computing (ICIVC)* (pp. 239-243). IEEE.
- [14] Gatys, L., Ecker, A., & Bethge, M. (2016). A Neural Algorithm of Artistic Style. *Journal of Vision*, 16(12), 326-342.
- [15] Fernandes, S. L., &Bala, G. J. (2018). Matching images captured from unmanned aerial vehicle. *International Journal of System Assurance Engineering and Management*, 9(1), 26-32.
- [16] Li, J., Jia, J., & Xu, D. (2018, July). Unsupervised Representation Learning of Image-Based Plant Disease with Deep Convolutional Generative Adversarial Networks. In *2018 37th Chinese Control Conference (CCC)* (pp. 9159-9163). IEEE.
- [17] Pathak, D., Krahenbuhl, P., Donahue, J., Darrell, T., &Efros, A. A. (2016). Context encoders: Feature learning by inpainting. In *Proceedings of the IEEE conference on computer vision and pattern recognition* (pp. 2536-2544).
- [18] Wang, X., & Gupta, A. (2016, October). Generative image modeling using style and structure adversarial networks. In *European Conference on Computer Vision* (pp. 318-335). Springer, Cham.
- [19] Wan, Q., & Panetta, K. (2016, May). A facial recognition system for matching computerized composite sketches to facial photos using human visual system algorithms. In *2016 IEEE Symposium on Technologies for Homeland Security (HST)* (pp. 1-6). IEEE.
- [20] Fernandes, S. L., &Bala, G. J. (2015). Match composite sketches with drone images. *IN2983/CHE/2015A*.
- [21] Klum, S. J., Han, H., Klare, B. F., & Jain, A. K. (2014). The FaceSketchID system: Matching facial composites to mugshots. *IEEE Transactions on Information Forensics and Security*, 9(12), 2248-2263.
- [22] Wang, Xiaogang, and Xiaou Tang. "Face photo-sketch synthesis and recognition." *IEEE Transactions on Pattern Analysis and Machine Intelligence* 31.11 (2008): 1955-1967.
- [23] Fernandes, S. L., &Bala, G. J. (2016). Self-Similarity Descriptor and Local Descriptor-Based Composite Sketch Matching. In *Proceedings of Fifth International Conference on Soft Computing for Problem Solving* (pp. 643-649). Springer, Singapore.
- [24] Bala, G. Josemin. "Developing a Novel Technique to Match Composite Sketches with Images Captured by Unmanned Aerial Vehicle." *Procedia Computer Science* 78 (2016): 248-254.
- [25] Vijayakumari, V. (2013). Face recognition techniques: A survey. *World journal of computer application and technology*, 1(2), 41-50.
- [26] Klum, S. J., Han, H., Klare, B. F., & Jain, A. K. (2014). The FaceSketchID system: Matching facial composites to mugshots. *IEEE Transactions on Information Forensics and Security*, 9(12), 2248-2263.
- [27] Blue Cross Blue Shield Blue Care Network. (n.d.). Retrieved September 12, 2019, from <https://www.bcbsm.com/health-care-fraud/fraud-statistics.html>.
- [28] Centers for Medicare & Medicaid Services. (2019, January 14) Retrieved September 12, 2019, from <http://www.cms.gov/Research-Statistics-Data-and-Systems/Monitoring-Programs/Medicare-FFS-Compliance-Programs/CERT>.
- [29] Nazeer, S. A., Omar, N., & Khalid, M. (2007, February). Face recognition system using artificial neural networks approach. In *2007 International Conference on Signal Processing, Communications and Networking* (pp. 420-425). IEEE.
- [30] Szegedy, C., Liu, W., Jia, Y., Sermanet, P., Reed, S., Anguelov, D., ...&Rabinovich, A. (2015). Going deeper with convolutions. In *Proceedings of the IEEE conference on computer vision and pattern recognition* (pp. 1-9).

- [31] Nakajima, H., Yanahara, H., Iwamoto, H., & Matsuyama, M. (2017). A deep convolutional deep neural network on an FPGA. In *Proceedings of the 2017 ACM/SIGDA International Symposium on Field-Programmable Gate Arrays* (pp. 290-290). ACM..
- [32] Liu, D., Peng, C., Wang, N., Li, J., & Gao, X. (2016, October). Composite face sketch recognition based on components. In *2016 8th International Conference on Wireless Communications & Signal Processing (WCSP)* (pp. 1-5). IEEE.
- [33] Lu, Y., Wu, S., Tai, Y. W., & Tang, C. K. (2018). Image generation from sketch constraint using contextual GAN. In *Proceedings of the European Conference on Computer Vision (ECCV)* (pp. 205-220).
- [34] Zhao, J., Xie, X., Wang, L., Cao, M., & Zhang, M. (2019). Generating Photographic Faces From the Sketch Guided by Attribute Using GAN. *IEEE Access*, 7, 23844-23851.